

## Spectroscopic properties of $\text{Eu}^{3+}$ -doped lithium sodium bismuth borate glasses for red luminescent optical devices

M. Parandamaiah, K. Naveen Kumar<sup>1</sup> and S. Venkatramana Reddy\*

Dept. of Physics, Sri Venkateswara University, Tirupati – 517 502, A. P., INDIA

<sup>1</sup>Dept. of Chemistry, Yeungnam University, Gyeongsan, Gyeongbuk - 712-749, Republic of Korea

\* Author for correspondence e-mail: drsvreddy123@gmail.com

---

**ABSTRACT** – The spectroscopic investigations of  $\text{Eu}^{3+}$ -doped lithium borate glasses in the  $60\text{B}_2\text{O}_3+20\text{LiF}+10\text{NaF}+10\text{Bi}_2\text{O}_3$  system for different concentrations of  $\text{Eu}^{3+}$  ions between 0.2 to 2 mol% are presented. We have successfully synthesized the above titled glasses doped with  $\text{Eu}^{3+}$  ions using melt quenching technique. Amorphous nature of the glass matrix has been confirmed from the XRD analysis. We have been analyzed the morphological and elemental analysis of the glass matrix by using SEM and EDAX profiles. Compositional, complex formation and ion-glass interactions were demonstrated from FTIR studies. Optical absorption studies have been systematically elucidated. Photoluminescence spectra show five prominent emission bands centered at 612, 577, 590, 651 and 701 nm corresponds to the  $^5\text{D}_0$  to several excited states under the excitation of 464 nm. Among all the concentrations of  $\text{Eu}^{3+}$  ions, at 1.5 mol%  $\text{Eu}^{3+}$  contained glass sample exhibit prominent red emission at 612 nm. Lifetime decay dynamics have been systematically analyzed for all the glasses. From the photoluminescence analysis, 1.5 mol%  $\text{Eu}^{3+}$  contained glass sample has been suggested as potential red luminescent glass matrix for several photonic device applications.

**Keywords** – Lithium sodium bismuth borate glasses-  $\text{Eu}^{3+}$ - Photoluminescence, SEM, EDXA and FTIR.

---

### 1. INTRODUCTION

In recent years, a noticeable attention has been focused on the rare earth ions doped glasses due to their wide variety of applications in various fields such as solid state lasers, flat panel displays planar waveguide, optoelectronic devices such as short wavelength (visible) lasers, display devices, sensors and high density frequency domain optical data storage [1]. Among various glasses, borate glasses are excellent host matrices because boric oxide ( $\text{B}_2\text{O}_3$ ) acts as a good glass former and flux material [2]. Borate glasses are structurally more intricate as compared to silicate or phosphate glasses due to two types of coordination of boron atoms with oxygens (3 and 4) and the structure of vitreous  $\text{B}_2\text{O}_3$  consists of a random network of boroxyl rings and  $\text{BO}_3$  triangles connected by B-O-B linkages. Moreover, the addition of a modifier oxide causes a progressive change of some  $\text{BO}_3$  triangles to  $\text{BO}_4$  tetrahedra and results in the formation of various cyclic units like diborate, triborate, tetraborate or pentaborate groups [3]. The glass containing heavy metal ions like  $\text{Bi}_2\text{O}_3$ ,  $\text{PbO}$ ,  $\text{PbF}_3$ , etc., borate glasses, decreases the host phonon energy and thereby improves the effective fluorescence [4] and also the addition of alkali fluoride ( $\text{NaF}$ ) minimizes the phonon energy of the host glass matrix [5]. Moreover, bismuth oxide contained host glass matrix improves chemical durability of the glass [6]. Despite, the  $\text{Bi}_2\text{O}_3$  is not a classical network former; it exhibits some superior physical properties like high density, high refractive index and exhibits high optical basicity, large polarizability and large nonlinear optical susceptibility [7]. The presence of two network forming oxides such as classical  $\text{B}_2\text{O}_3$  and the conditional  $\text{Bi}_2\text{O}_3$  glass former, the possible participation in the glass structure of both boron and bismuth ions with more than one stable coordination, the capability of the bismuth polyhedral and of the borate structural groups to form independent interconnected networks [8]. Many researchers have well known that the lithium is more electropositive ion. With the addition of lithium to the borate system, it causes drastic changes in binary lithium borate glass system. Hence, lithium glass forming ability over wide range of composition, higher bond strength, high transparency, low melting point and good rare earth ion solubility. Moreover, lithium borate glasses are useful for solid state battery applications [9, 10]. The luminescence of rare earth doped materials is due to the 4f-4f transitions. This luminescence is due to the shielding effect of the outer orbital (5s and 5p) on the 4f electrons and it results sharp absorption and emission spectral peaks may be observed [11].

The optical properties of  $\text{Eu}^{3+}$  ions doped in different host materials are highly sensitive to its environment characteristics and vary strongly from host to host. Among the various rare earth ions,  $\text{Eu}^{3+}$  ion is an efficient activator for rich red color center for display devices due to its dominant  $^5\text{D}_0 \rightarrow ^7\text{F}_2$  emission transition. The  $\text{Eu}^{3+}$  ion doped glasses are attracting a great deal of interest because of their persistent spectral hole burning can be

performed in the  ${}^7\text{F}_0 \rightarrow {}^5\text{D}_0$  transition of  $\text{Eu}^{3+}$  at ambient temperature and also these materials have potential use in high density optical storage devices [12]. In the present work, the optical absorption and photoluminescence spectral features of  $\text{Eu}^{3+}$  doped  $\text{B}_2\text{O}_3 + \text{LiF} + \text{NaF} + \text{Bi}_2\text{O}_3$  glass systems have been systematically studied for their utility in various optoelectronic and photonic devices.

## II. EXPERIMENTAL STUDIES

The host and  $\text{Eu}^{3+}$  doped lithium sodium bismuth borate (LSBiB) glass samples with compositions,  $(60-x) \text{B}_2\text{O}_3 + 20\text{LiF} + 10\text{NaF} + 10\text{Bi}_2\text{O}_3 + x\text{Eu}_2\text{O}_3$  (where  $x=0.2 \text{ mol.}\%$ ,  $0.4 \text{ mol.}\%$ ,  $0.6 \text{ mol.}\%$ ,  $0.8 \text{ mol.}\%$ ,  $1.0 \text{ mol.}\%$ ,  $1.5 \text{ mol.}\%$  and  $2.0 \text{ mol.}\%$  referred to as LSBiBEu02, LSBiBEu04, LSBiBEu06, LSBiBEu08, LSBiBEu10, LSBiBEu15 and LSBiBEu20 glasses respectively) were prepared by conventional melt quenching method using high purity precursor chemicals of boric acid ( $\text{H}_3\text{BO}_3$ ), bismuth oxide ( $\text{Bi}_2\text{O}_3$ ), lithium fluoride (LiF), sodium fluoride (NaF) and europium oxide ( $\text{Eu}_2\text{O}_3$ ) powders. About 10g batches of chemicals were mixed and ground in an agate mortar to attain homogeneous mixture. The mixture was taken into porcelain crucible and put into electric furnace at a temperature range of  $1050\text{--}1100\text{ }^\circ\text{C}$  for 45 min. Then the mixture was melted and air quenched by pouring it on a preheated brass plate. These samples were annealed at  $300\text{ }^\circ\text{C}$  for 3 h in order to remove strains. The density of glass samples was measured using Archimedes principle with xylene as an immersion liquid. The refractive indices were measured at  $589.3 \text{ nm}$  (sodium wavelength) using an Abbe refractometer with monobromonaphthalene as the contact liquid. For all the glass samples, the physical parameters like density, thickness, refractive index have been calculated.

The XRD spectral profiles of prepared glassy samples were obtained using SEIFERT 303 TT X-ray diffractometer with  $\text{CuK}_\alpha$  (line of  $1.5405 \text{ \AA}$ ), and it was operated at  $40 \text{ KV}$  voltage and  $50 \text{ mA}$  anode current. The FTIR spectrum of glass matrix was recorded using Thermo Nicolet IR200 spectrometer at Room temperature (RT) in the wavenumber range of  $3000\text{--}400 \text{ cm}^{-1}$ . Raman spectral profile was carried out at RT in the wavenumber range of  $1800\text{--}800 \text{ cm}^{-1}$  using LabRam HR 800 confocal Raman Spectrometer, which has Nd:YAG laser source ( $532.15 \text{ nm}$ ). Scanning electron microscopy (SEM-CARL ZEISS EVO MA 15) has been employed to investigate the morphological studies of the prepared glass samples. Optical absorption spectra were recorded using Perkin- Elmer Lambda 950 spectrophotometer in the wavelength range  $250\text{--}2500 \text{ nm}$ . The excitation and visible photoluminescence spectra (range  $400\text{--}900 \text{ nm}$ ) and decay spectral profiles of the  $\text{Eu}^{3+}$  doped glass matrices were recorded using JOBIN YVON Fluorolog- 3 fluorimeter using xenon flash lamp.

## III. RESULTS AND DISCUSSION

### 3.1. X-ray diffraction (XRD) and scanning electron microscopic (SEM) studies

The X-ray diffraction pattern of the above titled host glass shows no diffraction peaks and typical long range structural disorder which confirms the amorphous nature of the glass [13]. As the profile was similar in all the eight glasses, the one host glass (LSBiB) is shown in Fig.1.

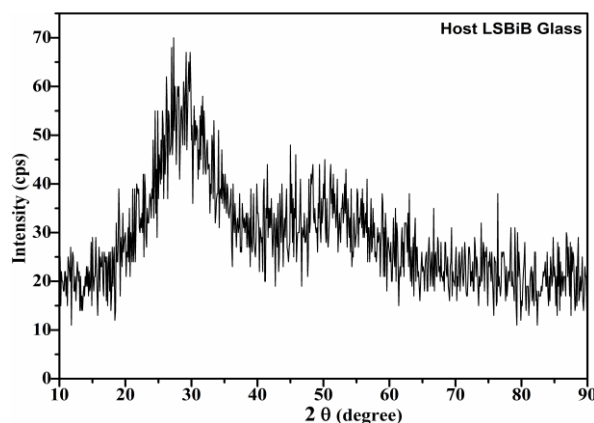


**Fig. 1** XRD profile of the host glass  $60\text{H}_3\text{BO}_3 + 20\text{LiF} + 10\text{NaF} + 10\text{Bi}_2\text{O}_3$  glass.

### 3.2 Scanning electron microscopy (SEM) studies

SEM image explores the smooth surface of the sample. This smooth surface indicates that the amorphous behavior of the glass matrix [14] and also we cannot identified any grain boundaries from the surface morphological image of the host LSBiBEu1.5 glass sample as shown in Fig. 2 (Left). The elemental analysis has been carried out from the EDAX spectral profile as shown in Fig. 2 (Right). The spectrum gives information about, the elements which are present in the investigated glass samples.

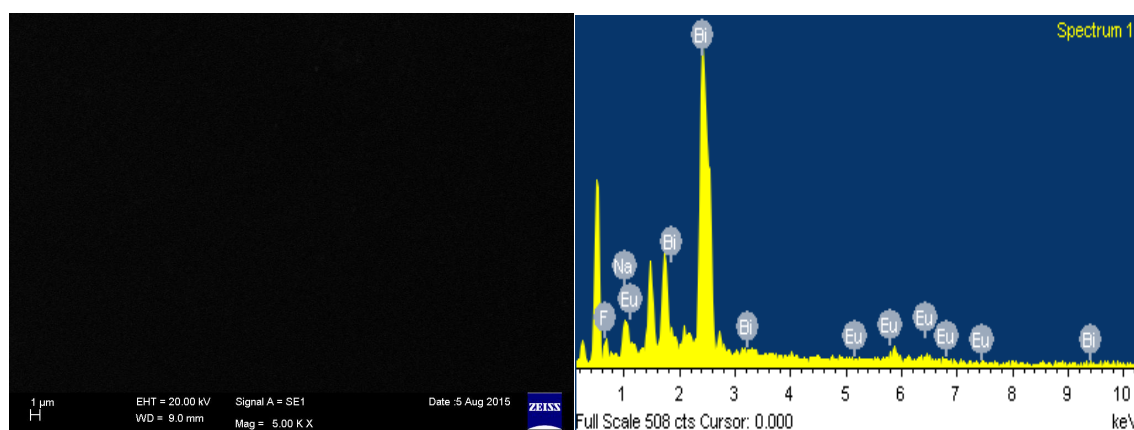


**Fig. 2** SEM (left) with EDAX (right) profiles of  $\text{Eu}^{3+}$  (1.5 mol%):  $60\text{H}_3\text{BO}_3+20\text{LiF}+10\text{NaF}+10\text{Bi}_2\text{O}_3$  glasses.

### 3.3 FTIR analysis

The FTIR spectrum of host  $\text{B}_2\text{O}_3+\text{LiF}+\text{NaF}+\text{Bi}_2\text{O}_3$  (LSBiB) glass is shown in Fig.3. The spectrum revealed characteristic peaks located at  $516\text{ cm}^{-1}$ ,  $667\text{ cm}^{-1}$ ,  $896\text{ cm}^{-1}$ ,  $1218\text{ cm}^{-1}$ ,  $1360\text{ cm}^{-1}$ ,  $1546\text{ cm}^{-1}$ ,  $1740\text{ cm}^{-1}$ ,  $2341\text{ cm}^{-1}$ ,  $3020\text{ cm}^{-1}$  and  $3732\text{ cm}^{-1}$ . The broad bands are due to combination of several factors such as high degeneracy of vibrational state, thermal broadening of lattice dispersion and mechanical scattering from the sample. The infrared bands are mainly related to  $\text{BO}_3$  and  $\text{BO}_4$  groups. The FTIR transmission band in the range of  $400\text{-}650\text{ cm}^{-1}$  is assigned to B-O-B bending vibrations as well as borate ring deformation [15]. It can be seen that the band at  $667\text{ cm}^{-1}$  is attributed to the bending vibration of the B-O-B linkage in the borate network, which had already reported in the earlier literature [16].

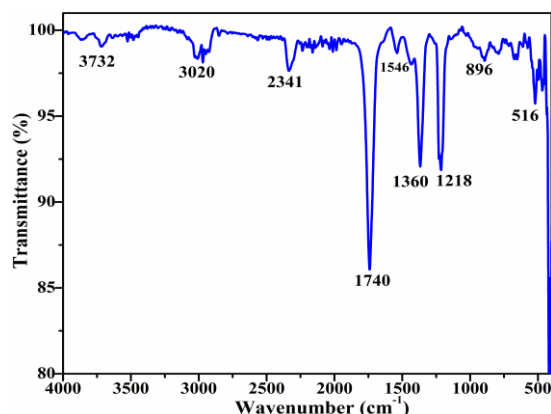


**Fig.3.** FTIR spectrum of the host glass  $60\text{H}_3\text{BO}_3+20\text{LiF}+10\text{NaF}+10\text{Bi}_2\text{O}_3$  glass.

It is also observed that the band observed at  $665\text{-}714\text{ cm}^{-1}$  is due to the B-O-B bending vibrations of  $\text{BO}_3$  triangles [17]. The band at around  $1360\text{ cm}^{-1}$  has been assigned to the stretching of trigonal  $\text{BO}_3$  units in meta, ortho and pyro-borate groups [18]. The band centered at  $986\text{ cm}^{-1}$  is assigned to B-O stretching vibrations of tetrahedral  $\text{BO}_4$  units in different borate groups. The band region from  $850\text{-}982\text{ cm}^{-1}$  is related to the symmetrical stretching vibration of  $\text{BO}_4$  units. The transmission band at  $1218\text{ cm}^{-1}$  is specific principle signature to the B-O stretching vibrations of  $\text{BO}_3$  triangular units with non-bridging oxygen atoms [19]. The FTIR spectral transmission peak observed in the region of  $2500\text{-}4000\text{ cm}^{-1}$  is attributed to water groups OH stretching vibrations.

### 3.4 Optical absorption studies

Figure 4 shows the absorption spectrum of  $\text{Eu}^{3+}$  doped LSBiB glass at room temperature. The spectrum reveals several absorption bands pertaining to  $\text{Eu}^{3+}$  ion due to transitions from its ground state multiplets such as  ${}^7\text{F}_0$  and thermally populated  ${}^7\text{F}_1$  levels to the upper levels of  ${}^4\text{F}_6$  configuration. As in the case of  $\text{Eu}^{3+}$  ions, the ground state  ${}^7\text{F}_0$  and the higher level  ${}^7\text{F}_1$  are very close to each other, so that at room temperature a significant amount of  ${}^7\text{F}_1$  levels are thermally populated.

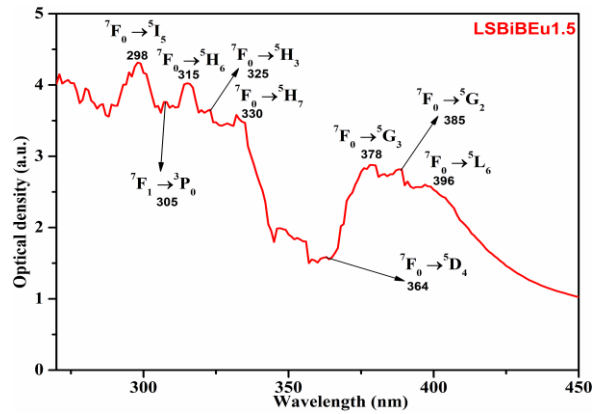


**Fig. 4** Optical absorption spectrum of the  $\text{Eu}^{3+}(1.5) : 60\text{H}_3\text{BO}_3+20\text{LiF}+10\text{NaF}+10\text{Bi}_2\text{O}_3$  glass.

The results in a characteristic absorption spectrum of  $\text{Eu}^{3+}$  ions exhibiting closely spaced doublets. In the present work, we have been obtained several absorption bands at 298nm, 305 nm, 315 nm, 330 nm, 364 nm, 378 nm, 385 nm and 396 nm. These absorption bands are assigned with corresponding electronic transitions  ${}^7\text{F}_0 \rightarrow {}^5\text{I}_5$ ,  ${}^7\text{F}_0 \rightarrow {}^3\text{P}_0$ ,  ${}^7\text{F}_0 \rightarrow {}^5\text{H}_6$ ,  ${}^7\text{F}_0 \rightarrow {}^5\text{H}_3$ ,  ${}^7\text{F}_0 \rightarrow {}^5\text{H}_7$ ,  ${}^7\text{F}_0 \rightarrow {}^5\text{D}_4$ ,  ${}^7\text{F}_0 \rightarrow {}^5\text{G}_3$ ,  ${}^7\text{F}_0 \rightarrow {}^5\text{G}_2$  and  ${}^7\text{F}_0 \rightarrow {}^5\text{L}_6$  respectively [20].

### 3.5 Photoluminescence studies

The excitation spectrum of the  $\text{Eu}^{3+}$  doped LSBiB glass monitored at 612 nm, within the most emission of europium is shown in Fig.5. It consist of several excitation bands originated from intra -4f forbidden transitions of  $\text{Eu}^{3+}$  ions at 362 nm, 381 nm, 394 nm, 413 nm, 464 nm, 525 nm, 532 nm and these bands are assigned with corresponding electronic transitions as ( ${}^7\text{F}_0 \rightarrow {}^5\text{D}_4$ ) at 362 nm, ( ${}^7\text{F}_0 \rightarrow {}^5\text{G}_2$ ) at 381 nm, ( ${}^7\text{F}_0 \rightarrow {}^5\text{L}_6$ ) at 394 nm, ( ${}^7\text{F}_0 \rightarrow {}^5\text{D}_2$ ) at 413 nm, ( ${}^7\text{F}_0 \rightarrow {}^5\text{D}_3$ ) at 464 nm, ( ${}^7\text{F}_1 \rightarrow {}^5\text{D}_1$ ) at 525 nm and ( ${}^7\text{F}_0 \rightarrow {}^5\text{D}_1$ ) at 532 nm [21]. From all these bands, the transition ( ${}^7\text{F}_0 \rightarrow {}^5\text{D}_3$ ) at 464 nm shows the prominent excitation intensity than the other bands. From the earlier reports, the 395 nm of major excitation has been reported in several reports for  $\text{Eu}^{3+}$  ions in various complexed materials. But here, we obtained an anomalous behavior which shows the 464 nm as major excitation for  $\text{Eu}^{3+}$  doped sample. It has been taken as optimized excitation band to excite the sample for emission spectral profiles.

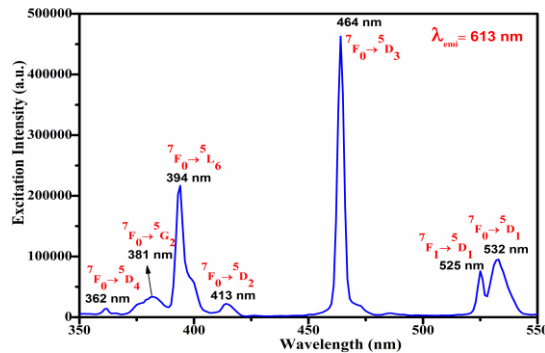


**Fig. 5** Excitation spectrum of the  $\text{Eu}^{3+} : 60\text{H}_3\text{BO}_3+20\text{LiF}+10\text{NaF}+10\text{Bi}_2\text{O}_3$  glass.

The luminescence characteristics have been carried out with the excitation wavelength of 464 nm as shown in Fig. 6. Several emission bands pertaining to  $\text{Eu}^{3+}$  ions are observed in the emission spectra of  $\text{Eu}^{3+}$  doped LSBiB glass. These excitation bands are assigned to corresponding electronic transitions such as ( ${}^5\text{D}_0 \rightarrow {}^7\text{F}_0$ ) at 577 nm, ( ${}^5\text{D}_0 \rightarrow {}^7\text{F}_1$ ) at 590 nm, ( ${}^5\text{D}_0 \rightarrow {}^7\text{F}_2$ ) at 612 nm, ( ${}^5\text{D}_0 \rightarrow {}^7\text{F}_3$ ) at 651 nm and ( ${}^5\text{D}_0 \rightarrow {}^7\text{F}_4$ ) at 701 nm [22]. From the emission spectra, strong emission is observed at 612 nm due to electric dipole transition  ${}^5\text{D}_0 \rightarrow {}^7\text{F}_2$  regarding  $\text{Eu}^{3+}$  ions in the glass matrix when excited with 464 nm. Remaining emission bands have also been assigned with corresponding electronic transitions and these bands are magnetic dipole allowed transitions. The forced electric dipole  ${}^5\text{D}_0 \rightarrow {}^7\text{F}_2$  transition is strongly hypersensitive to the environment of  $\text{Eu}^{3+}$  ions [23]. This indicates that the red emission is observed from the  $\text{Eu}^{3+}$  doped LSBiB glass sample under UV source and also under visible source. Here, we have obtained quite different result to traditional results for  $\text{Eu}^{3+}$  doped composite matrix. Significantly, we observed the greater emission intensity under visible excitation source (464 nm) than the UV source (Fig. 6).

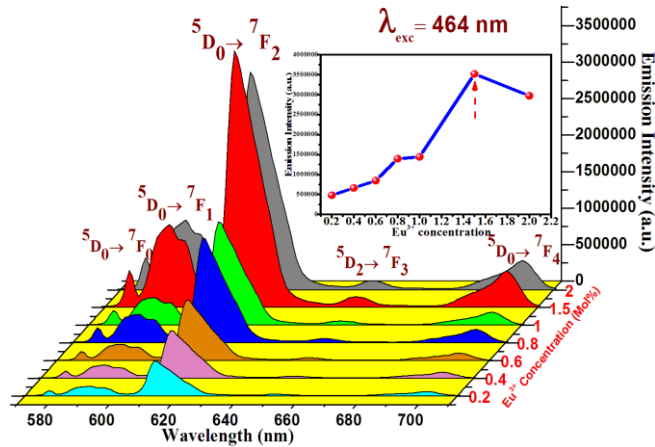


**Fig. 6** Emission spectra of  $\text{Eu}^{3+}$  (0.2, 0.4, 0.6, 0.8, 1, 1.5 and 2 mol%) :  $60\text{H}_3\text{BO}_3+20\text{LiF}+10\text{NaF}+10\text{Bi}_2\text{O}_3$  glasses under the excitation of 464 nm

It is also observed that the emission intensity has appreciably increases with increasing the  $\text{Eu}^{3+}$  ion concentration in the LSBiB glasses from 0.2 mol% to 1.5 mol%. Predominant emission feature has been observed at 1.5 mol% concentration of  $\text{Eu}^{3+}$  in LSBiB glass sample when compared to other prepared  $\text{Eu}^{3+}$  doped glasses. From this analysis, we have been identified the 1.5 mol% concentration is optimized concentration for  $\text{Eu}^{3+}$  doped LSBiB glass matrix for reddish emission. The emission intensities pertaining to  $\text{Eu}^{3+}$  doped LSBiB glass sample at 2 mol% concentration of  $\text{Eu}^{3+}$  has decreased as shown in inserted Fig. 6. This diminishing behavior of the emission intensities might be due to concentration quenching effect [24]. Figure 7 represents the schematic energy level diagram of  $\text{Eu}^{3+}$  doped LSBiB glasses.

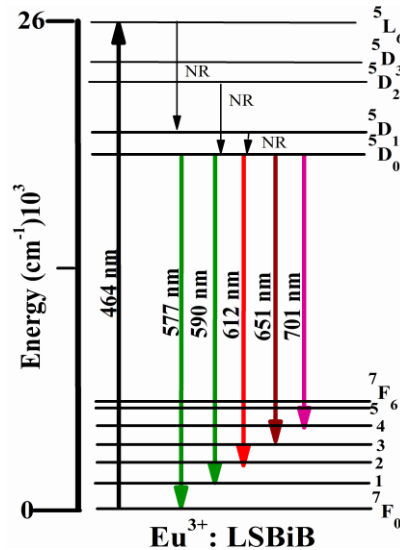


**Fig. 7** Schematic energy level diagram of the  $\text{Eu}^{3+}$  doped LSBiB glasses

### 3.5.1 Lifetime decay analysis

The lifetime of the  $^5\text{D}_0$  level, for all the glass samples with different concentrations of  $\text{Eu}^{3+}$  ions was measured by monitoring the fluorescence decay of  $^5\text{D}_0 \rightarrow ^7\text{F}_2$  transition under the excitation of two wavelengths such as 394 nm and 464 nm at room temperature. The characteristic decay curves have been found particularly for glass samples with 0.2, 0.4, 0.6, 0.8, 1, 1.5 and 2 mol% of  $\text{Eu}^{3+}$  concentrations are displayed in Fig. 8. The  $\text{Eu}^{3+}$  doped LSBiB glasses are found to be single exponential up to 1.5 mol%  $\text{Eu}^{3+}$  ion concentration and after that it becomes non-exponential due to the increase of  $\text{Eu}^{3+}$  ion concentration.

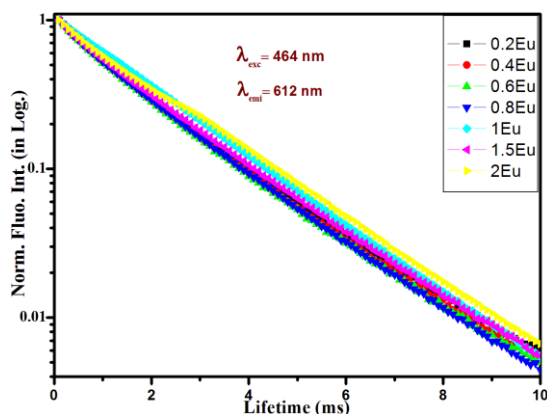


**Fig. 8.** Lifetime of the  $\text{Eu}^{3+}$  (0.2, 0.4, 0.6, 0.8, 1, 1.5 and 2 mol%) :  $60\text{H}_3\text{BO}_3+20\text{LiF}+10\text{NaF}+10\text{Bi}_2\text{O}_3$  glasses using 464 nm excitation and 612 nm emission.

In the present study, non-exponential behavior has been experienced for the 2 mol% of  $\text{Eu}^{3+}$  ions incorporated LSBiB glass due to concentration quenching effect of trivalent europium ions arising from ion-ion interaction [25]. There are two important mechanisms to explain energy transfer processes resulting in luminescence quenching. The first one is due to cross-relaxation between pairs of  $\text{Eu}^{3+}$  ions and another one is connected with the migration of excitation energy which can accelerate the decay by energy, transfer to the structural defects acting as energy sinks [26].

#### IV. CONCLUSIONS

In summary, it could be concluded that the optical glasses of  $(60-x)\text{B}_2\text{O}_3 + 20\text{LiF}+10\text{NaF}+10\text{Bi}_2\text{O}_3 + x\text{Eu}_2\text{O}_3$  (where  $x=0.2$  mol.%, 0.4 mol.%, 0.6 mol.%, 0.8 mol.%, 1.0 mol.%, 1.5 mol.% and 2.0 mol.%) have been synthesized by melt quenching method. The structural, morphological and compositional analysis of host glass has been demonstrated by XRD, SEM and FTIR studies. Optical absorption bands have been assigned with corresponding electronic transitions in absorption spectrum of  $\text{Eu}^{3+}$  (0.15 mol %) doped glass. From the photoluminescence studies,  $\text{Eu}^{3+}$  doped glasses exhibit a strong red emission at 612 nm, which are assigned with corresponding electronic transitions of  ${}^5\text{D}_0 \rightarrow {}^7\text{F}_2$  under the excitation of 464 nm at different concentrations of  $\text{Eu}^{3+}$  ions. Among all the  $\text{Eu}^{3+}$  doped glasses, 1.5 mol%  $\text{Eu}^{3+}$  doped glasses has shown an intense red emission. Based on the photoluminescence performances, the 1.5 mol% concentration of  $\text{Eu}^{3+}$  has been found to be optimized concentration for luminescent applications. The lifetime decay dynamics have also been systematically demonstrated. These  $\text{Eu}^{3+}$  ions doped optical glasses could be suggested as promising materials for red luminescent photonic devices.

#### References

- [1] D. Rajesh, A. Balakrishna, Y.C. Ratnakaram, Luminescence, structural and dielectric properties of  $\text{Sm}^{3+}$  impurities in strontium lithium bismuth borate glasses, *Optical Materials*, 35(2), 2012, 108–116.
- [2] M. Subhadra, P. Kistaiah, Infrared and Raman spectroscopic studies of alkali bismuth borate glasses: Evidence of mixed alkali effect, *Vibrational Spectroscopy*, 62(9), 2012, 23–27.
- [3] D.D. Ramteke, K. Annapurna, V.K. Deshpande, R.S. Gedam, Effect of  $\text{Nd}^{3+}$  on spectroscopic properties of lithium borate glasses, *J. Rare Earths*, 32(12), 2014, 1148–1153.
- [4] P. Srivastava, S. B. Rai, D. K. Rai, Optical properties of  $\text{Dy}^{3+}$  doped calibo glass on addition of lead oxide, *Spectrochim. Acta A: Molecular and Biomolecular Spectroscopy*, 59(14), 2003, 3303–3311.
- [5] P. Pascuta, L. Pop, S. Rada, M. Bosca, E. Culea, The local structure of bismuth borate glasses doped with europium ions evidenced by FT-IR spectroscopy, *Journal of Materials Science: Materials in Electronics*, 19(5), 2008, 424–428.
- [6] J.L. Doualan, S. Girard, H. Haquin, J.L. Adam, J. Montagne, Spectroscopic properties and laser emission of Tm doped ZBLAN glass at 1.8  $\mu\text{m}$ , *Optical Materials*, 24(3), 2003, 563–577.
- [7] S.P. Singh, R.P.S. Chakradhar, J.L. Rao, B. Karmakar, EPR, optical absorption and photoluminescence properties of  $\text{MnO}_2$  doped  $23\text{B}_2\text{O}_3-5\text{ZnO}-72\text{Bi}_2\text{O}_3$  glasses, *Physica B: Condensed Matter*, 405(9), 2010, 2157–2161.
- [8] P. Pascuta, G. Borodi, E. Culea, Influence of europium ions on structure and crystallization properties of bismuth borate glasses and glass ceramics, *J. Non-Cryst. Solids*, 354(53–54), 2008, 5475–5479.
- [9] R. S. Gedam, D. D. Ramteke, Electrical and optical properties of lithium borate glasses doped with  $\text{Nd}_2\text{O}_3$ , *J. Rare Earths*, 30(8), 2012, 785–789.
- [10] R. S. Gedam, D. D. Ramteke, Influence of  $\text{CeO}_2$  addition on the electrical and optical properties of lithium borate glasses, *J. Phys. Chem. Solids*, 74(10), 2013, 1399–1402.
- [11] G. Lakshminarayana, J. Qiu, M. G. Brik, I. V. Kityk, Photoluminescence of  $\text{Eu}^{3+}$ -,  $\text{Tb}^{3+}$ -,  $\text{Dy}^{3+}$ - and  $\text{Tm}^{3+}$ -doped transparent  $\text{GeO}_2\text{-TiO}_2\text{-K}_2\text{O}$  glass ceramics, *J. Physics: Condens. Matter*, 20(33), 2008, 335106 (1–11).
- [12] K. Vemasevana Raju, S. Sailaja, C. Nageswara Raju, B. Sudhakar Reddy, Optical characterization of  $\text{Eu}^{3+}$  and  $\text{Tb}^{3+}$  ions doped cadmium lithium aluminofluoroborate tellurite glasses, *Spectrochimica Acta Part A: Molecular and Biomolecular Spectroscopy*, 79(1), 2011, 87–91.

- [13] Yasser Saleh Mustafa Alajerami, Suhairul Hashim, Wan Muhamad Saridan Wan Hassan, Ahmad Termizi Ramli, Azman Kasim, Optical properties of lithium magnesium borate glasses doped with  $\text{Dy}^{3+}$  and  $\text{Sm}^{3+}$  ions, *Physica B: Condensed Matter*, 407(13), 2012, 2398–2403.
- [14] D. Rajesh, M. Dhamodhara Naidu, Y. C. Ratnakaram, A. Balakrishna,  $\text{Ho}^{3+}$ -doped strontium–aluminium–bismuth–borate glasses for green light emission, *Luminescence*, 29(7), 2014, 854–860.
- [15] N. A. El-Alaily, R. M. Mohamed, Effect of irradiation on some optical properties and density of lithium borate glass, *Mat. Sci. Eng. B*, 98(3), 2003, 193–203.
- [16] Chandrikam Gautam, Avadesh Kumar Yadav, Arbind Kumar Singh, A Review on Infrared Spectroscopy on borate glasses with Effects of Different Additives, *ISRN Ceramics Article ID 428497*, 2012, 1-17.
- [17] Safeya Ibrahim, Mohamed Mahmoud Gomaa, Hussein Darwish, Influence of  $\text{Fe}_2\text{O}_3$  on the physical, structural and electrical properties of sodium lead borate glasses, *J. Adv. Ceram.*, 3(2), 2014, 155-164.
- [18] Vandana Sharma, Supreet Pal Singh, Gurmel Singh Mudahar, Kulwant Singh Thind, Synthesis and Characterization of Cadmium Containing Sodium Borate Glasses, *New J. of Glass Ceram.*, 2(4), 2012, 150-155.
- [19] V. Simon, M. Spinu, R. Stefan, Structure and dissolution investigation of calcium-bismuth-borate glasses and vitroceraamics containing, *J. Mater. Sci. Mater. Med.*, 18, 2007, 507-512.
- [20] W. T. Camall, P. R. Fields and K. Rajnak, Electronic Energy Levels of the Trivalent Lanthanide Aquo Ions. IV.  $\text{Eu}^{3+}$ , *J. Chem. Phys.*, 49, 1968, 4450-4455.
- [21] Andreas Herrmann, Stefan Kuhn, Mirko Tiegel, Christian Rüssel, Fluorescence properties of  $\text{Eu}^{3+}$ -doped alumino silicate glasses, *Opt. Mater.*, 37, 2014, 293–297.
- [22] Kaushik Biswas, S. Balaji, Prantik Karmakar, K. Annapurna, Formation and spectral probing of transparent oxyfluoride glass-ceramics containing ( $\text{Eu}^{2+}$ ,  $\text{Eu}^{3+}$ : $\text{BaGdF}_5$ ) nano-crystals, *Opt. Mater.* 39, 2015, 153–159.
- [23] Peng Du, L. Krishna Bharat, Jae Su Yu, Strong red emission in  $\text{Eu}^{3+}/\text{Bi}^{3+}$  ions codoped  $\text{CaWO}_4$  phosphors for white light-emitting diode and field-emission display applications, *J. Alloys Compd.*, 633, 2015, 37–41.
- [24] Yu-Chun Li, Yen-Hwei Chang, Yu-Feng Lin, Yee-Shin Chang, Yi-Jing Lin, Synthesis and luminescent properties of  $\text{Ln}^{3+}$  ( $\text{Eu}^{3+}$ ,  $\text{Sm}^{3+}$ ,  $\text{Dy}^{3+}$ )-doped lanthanum aluminum germanate  $\text{LaAlGe}_2\text{O}_7$  phosphors, *J. Alloys Compd.*, 439, 2007, 367–375.
- [25] T. Grzyb, S. Lis, Structural and spectroscopic properties of  $\text{LaOF}:\text{Eu}^{3+}$  nanocrystals prepared by the sol–gel Pechini method, *Inorg. Chem.*, 50(17), 2011, 8112–8120.
- [26] C.R. Kesavulu, K. Kiran Kumar, N. Vijaya, Ki-Soo Lim, C.K. Jayasankar, Thermal, vibrational and optical properties of  $\text{Eu}^{3+}$ -doped lead fluorophosphate glasses for red laser applications, *Mater. Chem. Phys.*, 141(2), 2013, 903-911.